

## Structure and variability of spinning reaction waves in three-dimensional excitable media

Tatyana P. Ivleva\* and Alexander G. Merzhanov

*Institute of Structural Macrokinetics and Materials Science of Russian Academy of Sciences, 142432 Chernogolovka, Moscow region, Russia*

(Received 15 February 2001; published 28 August 2001)

A mathematical simulation for a reaction wave that propagates in a cylindrical sample is performed. The propagation modes that have not yet been observed experimentally are predicted. The areas of existence for these modes have been determined.

DOI: 10.1103/PhysRevE.64.036218

PACS number(s): 05.45.-a, 05.65.+b, 82.20.Wt

The nonlinear dynamics of excitable media is one of most interesting and fast-developing lines of research in modern science. Nonlinear dynamics manifests itself in spinning detonation [1,2], periodic chemical reactions [3,4], spinning combustion [5–8], and frontal polymerization [9]. In these cases, a zone of vigorous chemical reaction propagates along a spiral trajectory. Because of experimental difficulties, the inner structure of three-dimensional (3D) spinning waves remains unknown. Neither their front structure nor areas of their existence have not yet been properly determined by theoretical studies [10,11]. Some workers performed numerical two-dimensional (2D) investigation of spinning waves (e.g., see Refs. [12] and [13]). Such an approach neglects the radial heat transfer, which is inapplicable to continuous media. In particular, a 2D model describes combustion of a thin cylindrical shell. In this work, we took into account all three components of heat transfer (longitudinal, tangential, and radial ones), which allows us to describe the motion of hot spots inside a cylinder. Our numerical experiments show that the predicted [10,11] front structure turned out to be inadequate.

Let us consider the following physically clear model. During combustion, all reagents and products remain in their solid state, transfer coefficients are independent of temperature and degree of conversion, while the rate of heat release (reaction rate) obeys the first-order kinetic equation. In this case, we may use a widely adopted system of equations written in the cylindrical coordinates

$$c\rho_0 \frac{\partial T}{\partial t} = \lambda \left( \frac{\partial^2 T}{\partial r^2} + \frac{1}{r} \frac{\partial T}{\partial r} + \frac{1}{r^2} \frac{\partial^2 T}{\partial \varphi^2} + \frac{\partial^2 T}{\partial h^2} \right) + \rho_0 Q \frac{\partial \eta}{\partial t},$$

$$\frac{\partial \eta}{\partial t} = \begin{cases} k_0(1-\eta) \exp\left(-\frac{E_a}{RT}\right) & \text{for } \eta < 1, \\ 0 & \text{for } \eta \geq 1 \end{cases}$$

with the following boundary conditions:

$$t=0: \quad T=T_0, \quad \eta=0,$$

$$t>0, \quad r=r_0: \quad \lambda \frac{\partial T}{\partial r} = 0;$$

$$h=0: \quad \lambda \frac{\partial T}{\partial h} = 0,$$

$$h=h_0: \quad \begin{cases} T=T_w & \text{for } t=0, \\ \lambda \frac{\partial T}{\partial h} = 0 & \text{for } t < t_{ind}. \end{cases}$$

Here  $T$  is temperature,  $T_0$  is the initial sample temperature,  $T_w = T_0 + Q/c$  is the temperature attained in reaction;  $\eta$  is the conversion depth for a deficient component,  $\rho_0$  is the mean density;  $t$  is time,  $t_{ind}$  is the induction period;  $r, \varphi, h$  are the cylindrical coordinates;  $r_0, h_0$  are the radius and height of cylinder;  $c$  is the heat capacity;  $\lambda$  is the thermal conductivity;  $k_0$  is the pre-exponential factor;  $Q$  is the reaction heat;  $E_a$  is the activation energy for a given reaction; and  $R$  is the universal gas constant. Reaction is initiated at the upper face of the cylinder, so that it propagates downward.

Note that similar differential equations are being used in describing the electric conductivity, diffusion, magnetic conductivity, etc. Our calculation procedure for 3D modeling allowed us to solve the above system of equations by using only a PC. The obtained data provide an insight into the “inner” structure of a spinning wave.

The problem was solved (in the dimensionless form) by finite difference method by using a nonuniform grid. The spatial grid was nonuniform (with an unfixed number of nodes) and adaptable. In other words, in the zone of large gradients, the problem required many more grid points than outside the zone. As the gradients lowered, some of these points became unnecessary. A detailed procedure for constructing such grids is described in Ref. [14].

The spinning waves arise owing to the fact that the planar reaction front becomes unstable with respect to spatial perturbations. The range of system parameters within which the reaction front loses its stability is given by the following approximate expression (obtained upon numerical solution of the 1D problem [15]):

$$\alpha_{st} = 9.1 \frac{cRT_w^2}{E_a Q} - 2.5 \frac{RT_w}{E_a} < 1,$$

where  $\alpha_{st}$  is some combination of reaction parameters. For a given pair of reagents, the higher is  $\alpha_{st}$ , the higher is  $T_w$ .

\*Corresponding author; email: tanja@ism.ac.ru

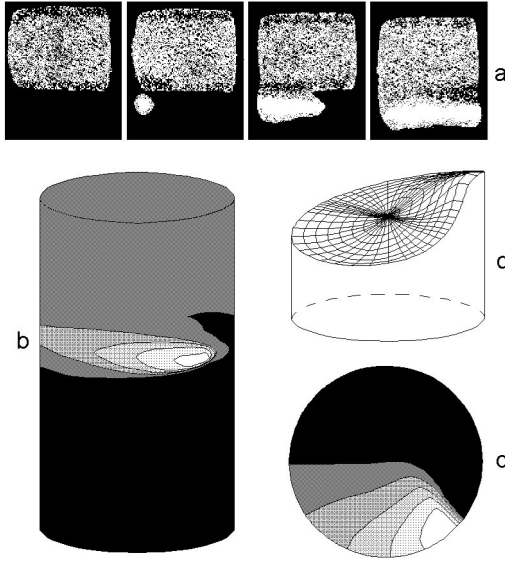


FIG. 1. Single-spot mode of steady spinning wave: (a) experimentally obtained image sequence for combustion of a cylindrical sample (see Ref. [5]) and our data for (b) temperature distribution over the sample surface, (c) reaction front structure, and (d) temperature distribution over a normal cross section at a point with maximum  $T$ . Brighter areas correspond to higher  $T$ ; in black areas,  $T < T_w$ .

In our calculations, we used  $\alpha_{st}$  and the dimensionless radius

$$R_0 = r_0 \left[ \frac{k_0 \rho_0 E_a Q}{\lambda R T_w^2} \exp\left(-\frac{E_a}{RT_w}\right) \right]^{1/2}$$

as governing parameters. The dimensionless radius  $R_0$  gives the number of reaction zones that could be stowed within the sample radius  $r_0$ .

Generally, spinning reaction waves manifest themselves as one or several bright hot spots that move alongside a screw trajectory over the sample surface [5–8]. (A hot spot is a zone where the reaction rate is maximal and where  $T$  is much greater than  $T_w$ .) The so-called single-spot spinning wave is most widespread [Fig. 1(a)]. However, the structure of the reaction wave and subtle details of its propagation remained unclear because of serious difficulties encountered in experiments (inapplicability of optical methods, perturbations introduced by thermocouples and other probes) and calculations (strong nonlinearity caused by the exponential dependence of reaction rate on temperature).

In the simplest case (Fig. 1), the process develops steadily: the front profile remains permanently curved and just propagates downward alongside a screw trajectory at a constant velocity. Spinning waves with two spots on the surface are also possible. According to our calculations, these waves emerge in cylindrical samples with a relatively small  $R_0$ . With increasing  $R_0$ , the spinning waves lose their stability: although remaining periodic, they undergo numerous transformations during one period. The motion of hot spots in different modes is illustrated in Fig. 2.

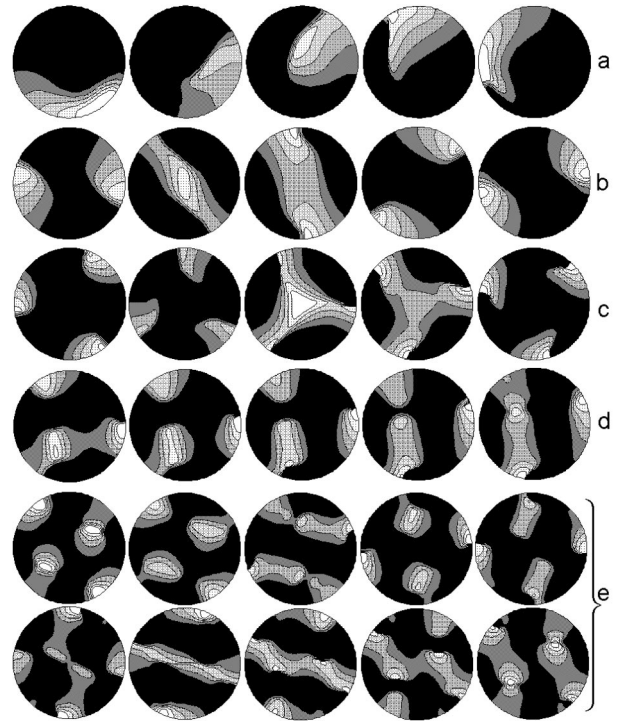


FIG. 2. Image sequences illustrating one period of the motion of hot spots at different  $R_0$  for  $\alpha_{st} \approx 0.9$ : (a) unsteady single-spot wave ( $R_0=60$ ), (b) unsteady symmetric two-spot wave ( $R_0=40$ ), (c) unsteady symmetric three-spot wave ( $R_0=80$ ), (d) asymmetric flickering wave ( $R_0=60$ ), and (e) unsteady multi-spot wave ( $R_0=80$ ). Temperature distribution is shown for a normal cross section at a point with a maximum value of  $T$ . Sample cross sections are normalized to equal size (irrespective of real value of radius  $R_0$ ). Brighter areas correspond to higher  $T$ ; in black areas,  $T < T_w$ .

With an increase in  $R_0$ , the wave propagation becomes periodic but unsteady. Our data show that, for an unsteady single-spot spinning wave [Fig. 2(a)], the spot size, velocity of motion alongside the screw trajectory, and temperature also undergo pulsation. When the hot spot is extended, it reaches the central area (i.e., temperature at the center increases) and then shrinks again (temperature at the sample center goes down) [Fig. 2(a)]. As a result,  $T$  and instantaneous wave velocity at the sample axis oscillate around some mean value. Such a pulsation was observed experimentally [16]. When the hot spot shrinks (toward the surface), a heat flux from the spot is insufficient for initiating the reaction at the sample axis (because  $R_0$  is relatively large). But instead, a zone of heat-affected mixture is formed. As the hot spot approaches this zone, it initiates the reaction front in this zone. Depending on  $\alpha_{st}$  and  $R_0$ , a maximum value of  $T$  may be attained at any point of the front, including the sample center. When reaction is completed in the center, the hot spot shrinks toward the sample surface, to the areas with still unreacted mixture. In this way, the spot structure and velocity of its motion undergo periodic changes (not multiple of  $2\pi$ ).

A simplest symmetric spinning wave comprises two diametrically opposite hot spots. Their motion may be accompanied either (i) by steady propagation along the sample axis

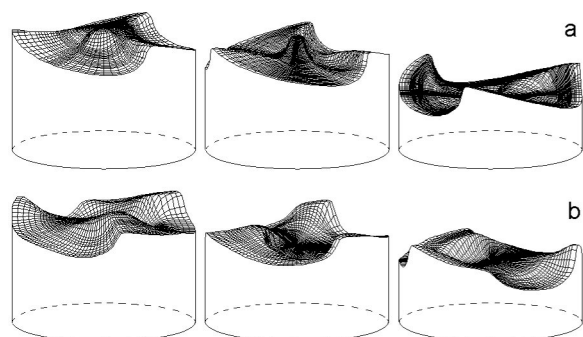


FIG. 3. Image sequences showing the evolution of reaction front: (a) unsteady symmetric three-spot wave and (b) unsteady asymmetric three-spot wave.

(for small  $R_0$  and insignificant deviation from the stability limit) or (ii) by pulsating reaction in the central area. In the latter case, the motion of hot spots becomes unsteady [Fig. 2(b)]. Propagation of hot spots over the surface gradually decelerates until fast burning (flare) of preheated mixture in the central area. This is followed by the transfer of released heat to the near-surface areas, which increases the reaction rate at the surface. With increasing separation from the hot central zone, the temperature of hot spots and their velocity decrease again. The process is repeated periodically.

We observed similar spinning waves with three hot spots. In this case [Fig. 2(c)], the temperature of spots simultaneously decreases, while the central area is heated (by heat transfer) until a flare that raises the temperature of the surface spots. With increasing  $T$ , the spots begin to move faster, and *vice versa*.

The evolution of front structure during one period is illustrated in Fig. 3(a). It follows that the reaction front in the center gradually retards while the area of retardation becomes narrower. In the third period, the front structure becomes identical to the initial one (although shifted along  $z$  and  $\varphi$ ).

There also exists another three-spot mode — the asymmetric one. In this case, three spots alternatively leave the surface toward the sample center. The spot that is inside coalesces with one of two near-surface spots, thus giving rise to two new spots. One of these two spots appears at the surface, while another moves toward the third one [Fig. 2(d)]. As a result, we observe three spots that alternatively flare and fade on the surface. The evolution of reaction front is illustrated in Fig. 3(b).

In the case of the multispot wave — a most complicated of observed propagation modes — the spots are periodically taken off (in pairs) from the surface and move toward the sample center. In this case, they interact each with the other

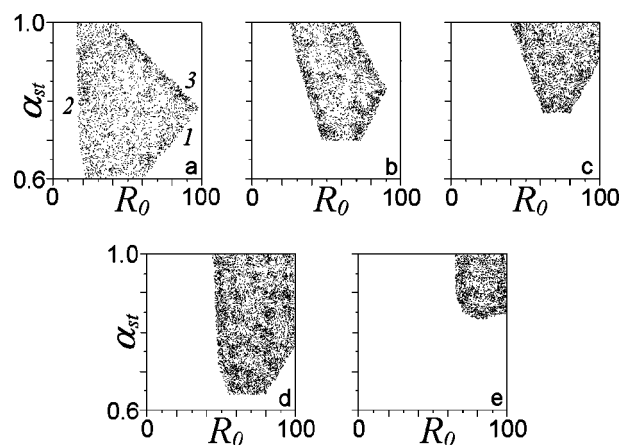


FIG. 4. The region of existence for (a) single-spot wave, (b) symmetric two-spot wave, (c) symmetric three-spot wave, (d) asymmetric three-spot wave, and (e) multi-spot flickering wave.

as well as with the spots that remain in the near-surface layer, which is accompanied by bright flaring or fading. The spots bifurcate and then merge [Fig. 2(e)].

We found that several propagation modes may correspond to identical  $\varphi$  and  $R_0$ . The type of established propagation mode depends on the conditions of initiation. The approximate ranges of existence for different propagation modes are given in Fig. 4.

Nevertheless, our data seem to be considerably meaningful. For example, let us consider the case of a single-spot wave. The overall view of the process becomes markedly complicated with increasing  $R_0$  and decreasing  $\alpha_{st}$ . This explains the appearance of curve 1 in Fig. 4. For small  $R_0$ , the reaction front is planar when the sample diameter is smaller than the width of three preheated zones (see curve 2 in Fig. 4). Propagation modes with a poorly developed front structure are rearranged more readily, as may be inferred from the existence of curve 3 in Fig. 4. The lower limit for the range of existence may be related to some difficulties encountered in establishing a given propagation mode.

We believe that our data shed new light on the mechanism of spinning detonation in gases, periodic chemical reactions, spinning combustion in solid–solid and solid–gas systems, and frontal polymerization. These data may also turn out to be useful for researchers active in biological studies, geology, ecology, and other areas of modern science and technology.

#### ACKNOWLEDGMENTS

We are grateful to Professor I. P. Borovinskaya for fruitful discussions and advice.

- [1] C. Campbell and D. W. Woodhead, *J. Chem. Soc.* **129**, 3010 (1926).  
 [2] C. Campbell and D. W. Woodhead, *J. Chem. Soc.* **130**, 1572 (1927).

- [3] T. Amemiya *et al.*, *Phys. Rev. Lett.* **77**, 3244 (1985).  
 [4] Z. Nădy-Ungvarai, J. Ungarai, and S. C. Muller, *Chaos* **3**, 15 (1993).  
 [5] A. G. Merzhanov, A. K. Filonenko, and I. P. Borovinskaja,

- Sov. Phys. Dokl. **208**, 122 (1973).
- [6] Yu. M. Maksimov *et al.*, *Combust., Explos. Shock Waves* **15**, 415 (1979).
- [7] S. Zhang and Z. A. Munir, *J. Mater. Sci.* **27**, 5789 (1992).
- [8] J. Puszynski *et al.*, *Z. Naturforsch., A: Phys. Sci.* **43A**, 1017 (1988).
- [9] J. Masere *et al.*, *Chaos* **9**, 315 (1999).
- [10] G. Sivashinsky, *SIAM (Soc. Ind. Appl. Math.) J. Appl. Math.* **40**, 432 (1981).
- [11] J. J. Thiart *et al.*, *Combust. Sci. Technol.* **82**, 185 (1992).
- [12] T. P. Ivleva, A. G. Merzhanov, and K. G. Shkadinsky, *Sov. Phys. Dokl.* **23**, 255 (1978).
- [13] A. Bayliss and B. J. Matkovsksky, *Physica D* **128**, 18 (1999).
- [14] T. P. Ivleva and K. G. Shkadinsky, *Inf. Byull. Gosfonda Algoritmov i Programm USSR*, **1**, 18 (1979).
- [15] K. G. Shkadinsky, B. I. Khaikin, and A. G. Merzhanov, *Combust., Explos. Shock Waves* **1**, 15 (1971).
- [16] A. V. Dvoryankin and A. G. Strunina, *Fiz. Goreniya Vzryva* **2**, 41 (1991).